engineering proceedings

Proceedings

3D Printable Piezoelectric Composite Sensors for Guided Ultrasonic Wave Detection †

Thomas Roloff [1,*], Rytis Mitkus [1], Jann Niklas Lion [1] and Michael Sinapius [1]

1 Technische Universität Braunschweig, Institute of Mechanics and Adaptronics; thomas.roloff@tu-braunschweig.de
* Correspondence: thomas.roloff@tu-braunschweig.de; Phone: +49 531 8069
† Presented at the 8th Electronic Conference on Sensors and Applications, 1–15 November 2021; Available online: https://ecsa-8.sciforum.net/.

Citation: Roloff, T.; Mitkus, R.; Lion, J. N.; Sinapius, M. 3D Printable Piezoelectric Composite Sensors for Guided Ultrasonic Wave Detection. *Eng. Proc.* **2021**, *1*, 0. https://doi.org/

Received:
Accepted:
Published:

Abstract: Commercially available photopolymer resin is combined with Lead Zirconate Titanate (PZT) micrometer size piezoelectric particles to form 3D printable suspensions that solidify under UV light. This in turn allows achieving various non-standard sensor geometries which might bring benefits, such as increased piezoelectric output in specific conditions. However, it is unclear whether piezoelectric composite materials are suitable for Guided Ultrasonic Wave (GUW) detection which is crucial for Structural Health Monitoring (SHM) in different applications. In this study, thin piezoelectric composite sensors are tape casted, solidified under UV light, covered with electrodes, polarized in a high electric field and adhesively bonded onto a waveguide. This approach helps to understand the capabilities of thin piezoelectric composite sensors for GUW detection. In an experimental study, thin 2-dimensional rectangular, circular and annulus segment shaped piezoelectric composite sensors with an effective surface area smaller than 400 mm^2 applied to an aluminum plate with a thickness of 2 mm demonstrate successful detection of GUW up to 250 kHz. An analytical calculation of the maximum and minimum amplitude for the ratio of the wavelength and the sensor length in wave propagation direction shows good agreement with the sensor recorded amplitude. The output of the piezoelectric composite sensors is compared to commercial piezoelectric discs to evaluate their performance.

Keywords: piezocomposite sensor, structural health monitoring, guided ultrasonic waves, sensor geometry

1. Introduction

In the emerging field of Structural Health Monitoring (SHM) for large plate-like and complex thin-wall structures, Guided Ultrasonic Waves (GUW) are state of the research to detect damages and evaluate the condition of the structure. GUW interfere with structural changes e.g. stringers which leads to a complex wave field. To guarantee reliable measurements, direction sensitive actuation and sensing is under investigation [1, p.359ff.], [2]. Direction sensitivity is closely connected to the sensor size and dimensions [1, p.359ff.]. Therefore the idea is, that the shape of the sensor has an influence on the GUW detection, too. Manufacturing methods such as 3D printing or tape casting allow almost free-form design of piezoelectric composite sensors that are solidified with UV light from suspensions made of PZT particles dispersed in a photopolymer resin. Application-specific free-form designed, variable, direction and mode sensitive sensors could lead to a major extension of existing SHM setups.

GUW are dispersive waves that appear in structures with two parallel free surfaces. They occur in symmetric and asymmetric modes and show displacements inside and on the surface of a structure. The particles perform in-plane and out-of-plane movements [3], [4, p.198ff.]. GUW are well suited for SHM applications due to their low damping over long distances [5, p.6].

Solid piezoceramic discs are state of the art for GUW detection [4, p.239ff.], but other piezoelectric materials exist, e.g. piezoelectric polymers or piezocomposite materials. Pure piezoceramics are stiff and brittle, can not be applied on curved surfaces and often cause high reflections of GUW due to their high acoustic impedance [6]. Piezoelectric photopolymers, like polyvinylidene fluoride (PVDF), are very flexible but offer a low electromechanic coupling and sensitivity. The aim of piezoelectric composite materials is to combine the advantages of both.

One of the first mentions of piezoelectric composites in the field of SHM applications in the literature was Giurgiutiu and Lin in 2004 [7] with the in-situ fabrication of piezoelectric wafer active sensors (PWAS) using a piezoelectric composite approach. Additive manufacturing methods of flexible piezoelectric composites are rarely mentioned in the SHM field. Investigations on 3D-printed piezoelectric composites are undertaken, but mostly in other subject fields (e.g. energy harvesting and ultrasonic or biomedical imaging) [8], [9]. In most cases, the piezoelectric material PZT is used because of the very high piezoelectric properties compared to most piezoelectric materials ($d_{33,PZT} = 225 - 590\,\mathrm{pC\,N^{-1}}$) [10]. In particular, polymer- [11], [12] and cement-based matrices [13] are used as the inactive phase of the composite.

However, the effect of the sensor geometry was not investigated, but modifications are possible just as mode-selective and directive actuators and sensors, e.g. sensor setups with interdigital electrodes [2]. The mode-selectivity and directivity is strongly connected to the sensor geometry [1, p.359ff.]. This fact will be described briefly in the following paragraph to give the basics for the evaluation in Section 3.

When idealized as a plate capacitor, the generated voltage by a piezoelectric sensor under mechanical deformation can be calculated as follows:

$$U = \frac{d_{31} t_s Y_s}{\varepsilon_{33}^{\sigma} 2a2b(1-\nu)} \iint_A (\varepsilon_x + \varepsilon_y)\, dx\, dy. \tag{1}$$

where d_{31} denotes the piezoelectric charge coefficient, t_s the sensor thickness, $2a$ the sensor length, $2b$ the sensor width, Y_s the Young's modulus of the sensor, $\varepsilon_{33}^{\sigma}$ the dielectric constant at constant mechanical stress, ν the Poisson's ratio and ε_x and ε_y the strains on the surface of the structures [2, p.21f.] [14].

In the following consideration a planar, one-dimensional Lamb wavefield is assumed, generating strain in x-direction on the plate surface. All parameters except the sensor length are kept and the sensor is assumed to be a 1D piezoelectric resonator. Then the first amplitude maximum and minimum for the different modes occur at the following wavelengths λ, with a detailed description in [2, p.21f.] and [4, p.249ff.]:

$$\text{First sensor amplitude maximum at: } \lambda = 4a, \tag{2}$$

$$\text{First sensor amplitude minimum at: } \lambda = a. \tag{3}$$

The previous statements show, that the sensor performance (i.e. maximum voltage generated) depends on multiple parameters with size and geometry playing a key role. With the assumption of a 1D wavefield and a 1D resonator it can be seen that the ratio between the wavelength and the sensor length is crucial for the generated signal amplitude of a piezocomposite sensor under GUW excitation.

This study experimentally investigates the applicability of piezoelectric composite sensors for GUW detection and their geometry dependency of the signal generation under GUW excitation. GUW detection in an isotropic medium up to a frequency-thickness ratio of at least $fd = 0.5\,\mathrm{MHz\,mm}$ is proven and it is shown, that the geometry of the sensor and sensor orientation with respect to the wave propagation direction play a key role in the sensor behavior.

2. Materials and Methods

2.1. Sensor manufacturing

The suspensions used to manufacture sensors throughout this study consist of 20 vol% PZT particles (PIC225, particle size 1.6 µm, *PI Ceramic, Germany*) dispersed randomly in a photopolymer resin (*High Temperature resin V2, Formlabs, USA*) with a centrifugal mixer (*Speedmixer DAC 700.2 VAC-P, Hauschild BmbH & Co. KG, Germany*). Materials are selected based on our previous studies [15]. No solvents or any other additives are used in suspension preparation. To achieve proper dispersion of the particles, the suspension is mixed under vacuum (20 mbar) for three times with the following parameters: 1 min at 900 min^{-1}, 0.5 min at 1250 min^{-1} and 4 min at 1750 min^{-1}. Dispersion quality is proven with SEM imaging. Because of the high density of PZT particles compared to the photopolymer ($\rho_{PZT} = 7.85\,\text{g}\,\text{cm}^{-3}$, $\rho_{photopolymer} = 1.14\,\text{g}\,\text{cm}^{-3}$), the suspension sediments in 24 h. Therefore, the suspension is remixed each time before sensor manufacturing.

Sensors are manufactured by tape casting. A PVC foil sticker (*Oraguard 270G*, thickness 150 µm), with the required sensor geometry pre-cut by a plotter, is glued on glass. The suspension is filled on the sticker and tape casted manually with a metal blade held at 30° from vertical position. The glass with tape casted sensors is placed 50 mm below a UV light source (*EQ CL30 LED Flood 405, Loctite)* for 60 s for solidification.

Five individual measurements along the sensor surface are used to determine the respective sensor thicknesses required for dielectric measurements and polarization. Another pre-cut PVC sticker with electrode geometry (1 mm offset from outer edges of the sensor) is adhered onto the sensor. Silver coated copper (*843AR Super Shield Silver Coated Copper Conductive Coating, MG Chemicals*) is sprayed manually in two thin layers as an electrode. After drying, the sticker is peeled off, leaving the electrode on the sensor and the same procedure is repeated on the other side.

To polarize the sensors, a 55 $\text{kV}\,\text{mm}^{-1}$ DC electric field is applied for 21 min in total (4 min ramp up, 16 min hold, 1 min ramp down) in a warm silicone oil at 65 °C. After polarization, the sensors are dried with a paper towel and are left for a minimum of 24 h to dry further. Conductive silver ink (*Silber-Leitlack, Busch GmbH & Co. KG, Germany*) is used on the corner of each sensor to generate a single side access to both electrodes and ensure full and even sensor adhesion to the aluminum waveguide.

2.2. Sensor geometry selection

For comparability, the sensors electrode surfaces are set to 324 mm^2. The overall size of the sensors with different geometries may vary due to the 1 mm offset. The mean sensor thickness is 129.9 µm and the average electrode thickness is 44.3 µm. In addition to conventional geometries (square and circle), the more complex geometry of an annulus segment is investigated. Its radii are adapted to the expected propagating wavefront of a circular actuator. Figure 1 shows the respective sensor geometries and a commercial circular piezoceramic sensor in respective orientation to the wave propagation direction.

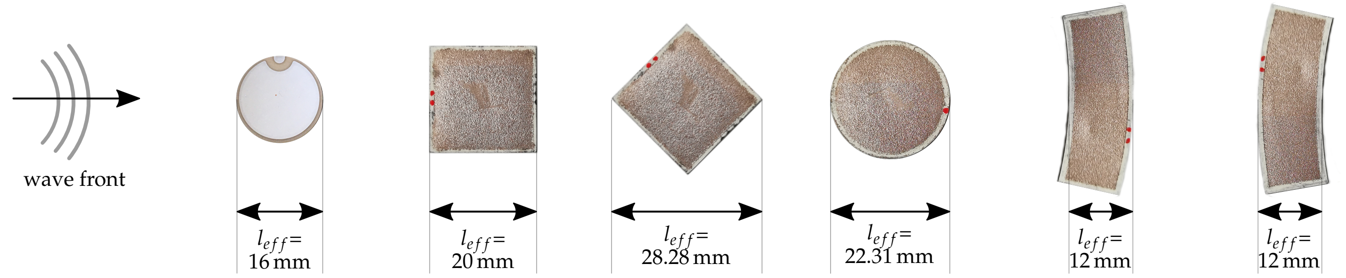

(a) Wave front of a circular wave field **(b)** Commercial Piezoceramic PRYY-1126 **(c)** Sensor shape: square Orientation: 1 **(d)** Sensor shape: square Orientation: 2 **(e)** Sensor shape: circle Orientation: - **(f)** Sensor shape: annulus seg. Orientation: 1 **(g)** Sensor shape: annulus seg. Orientation: 2

Figure 1. Sensor shapes under investigation with regard to the wave propagation direction and assumptions concerning the effective sensor length in wave propagation direction

2.3. Determination of detectable GUW signals

The test setup is shown in Figure 2. A square aluminum plate (material 3.3535) with an area of 1 m × 1 m and a thickness of 2 mm is used as a waveguide. A piezoceramic disc actuator PRYY-1126 from *PI Ceramic GmbH* (material: PIC255, diameter 16 mm, ceramic height: 200 µm) is used for excitation and adhesively bonded to the center of the plate with cyanoacrylate. Due to the circular ceramic, the wavefield is assumed to have a concentrically propagating circular wave front. The sensors are equally glued to the aluminum plate in a circular arrangement with the sensors geometric center on a circle with a radius of 156 mm around the actuator. The sensors under investigation will be placed in two orientations with respect to the wavefront except for the circular ones, see Figure 1. A PicoScope 5442B is used in combination with a laptop to serve as a signal generator to provide the excitation signal and the amplification is realized using a high voltage amplifier *WMA-300* by *Falco Systems*. The laptop with the PicoScope also acquires the measurement data.

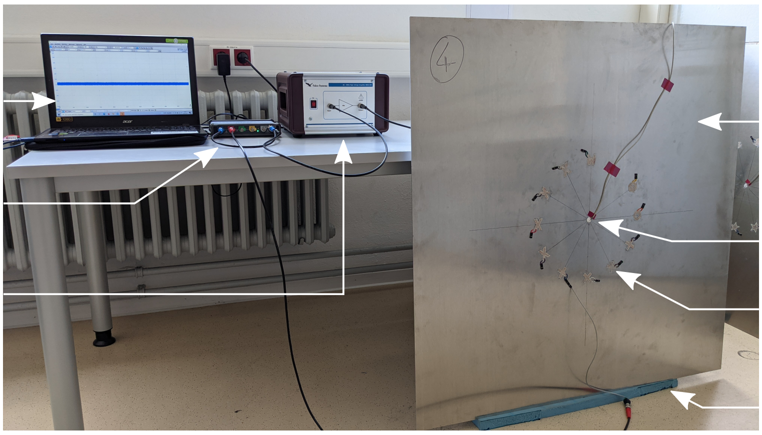

Figure 2. Test setup to determine the peak-to-peak voltage of the sensors under GUW excitation

For excitation, a 5-cycle, hanning-windowed sine burst is used. The investigated burst center frequencies range from 5 kHz to 200 kHz with an interval of 5 kHz and from 200 kHz to 250 kHz with an interval of 25 kHz. Due to the short distance between the actuator and the sensors, no temporal separation of the S_0 and A_0 modes is possible. Therefore, the peak-to-peak voltage amplitude U_{pp} is measured in a time window from the calculated start of the faster S_0 to the end of the slower A_0 mode. To generate comparable sensor signals, a normalization is performed. The signals are normalized using the sensors thicknesses, a factor to compensate the capacity loss due to polarization errors and a factor to compensate for the amplifier behaviour, as the amplification factor decreases with increasing frequency depending on the capacitive load.

3. Results and discussion

The results for the sensors shown in Figure 1, manufactured and measured as described in Section 2, are presented in Figure 3. According to Equations 2 and 3 and the assumption of a 1D wave propagation, the expected frequencies/wavelengths for a maximum or minimum amplitude for a given sensor length are calculated and shown as solid and dotted vertical lines, respectively. Figure 1 shows the assumed effective sensor lengths in wave propagation direction. The frequency dependent wavelengths of the wave guide are calculated using the *Dispersion Calculator* developed at the *German Aerospace Center* (DLR). The results generally show that GUW detection with piezocomposite sensors is possible.

The commercially available piezoceramic sensor shows higher amplitudes than the custom composite sensors over the whole investigated frequency range. This is due to a higher thickness (see Equation 1, $h_{PRYY-1126} = 200\,\mu m$, $h_{piezocomposite} = 129.9\,\mu m$), stiffness (see Equation 1) and piezoelectric charge coefficient (see Equation 1). The coefficient of the commercial PRYY-1126 ($d_{31,PRYY-1126} = -180\,\mathrm{pC\,N^{-1}}$ [6]) is approx. 70 times higher than the one of the piezocomposite sensor ($d_{31,piezocomposite} \approx -2.5\,\mathrm{pC\,N^{-1}}$). The maxima of the annulus segment shaped sensor are higher than for the standard geometries (circular and square shape). This might give the impression that a short effective sensor length leads to higher amplitudes, but the square shaped sensor shows higher amplitudes for orientation 2 with a higher effective sensor length than in orientation 1. Furthermore, for the annulus segment shaped sensor, the ones in orientation 2 show better performance. Therefore, further investigations of the influence of the 2D geometry rather than only the effective sensor length of the sensors are necessary and could lead to an improvement of the sensor design.

The analytical results for the expected maximum and minimum amplitudes fit well with the measurements of the annulus segment shaped sensor and the square shape one in orientation 1. The two circular sensors show slight deviations from the calculated extrema and the results of the rotated square sensor (orientation 2) deviate most from the analytical calculations. Possible reasons are erroneous material properties in the analytical solution, a superposition of the A_0 and S_0 mode as the group velocities do not differ enough for wave package separation and most likely a wrong estimation of the effective sensor length. Furthermore, the two measurements for the square sensor in orientation 2 differ considerably from another. This shows, that more profound investigations are necessary to reliably characterize the different sensors.

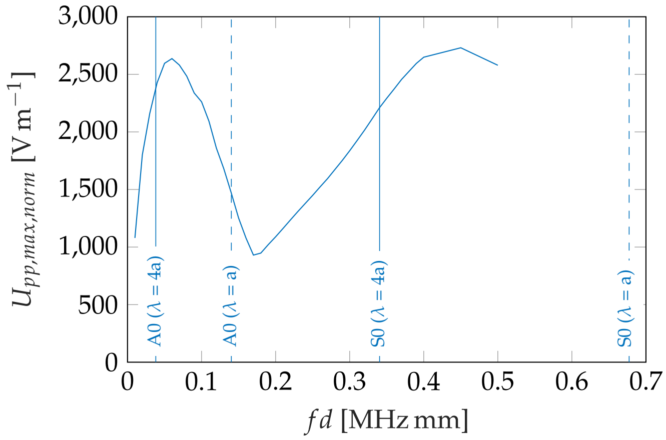

(a) Commercial solid piezoceramic sensor, Figure 1b

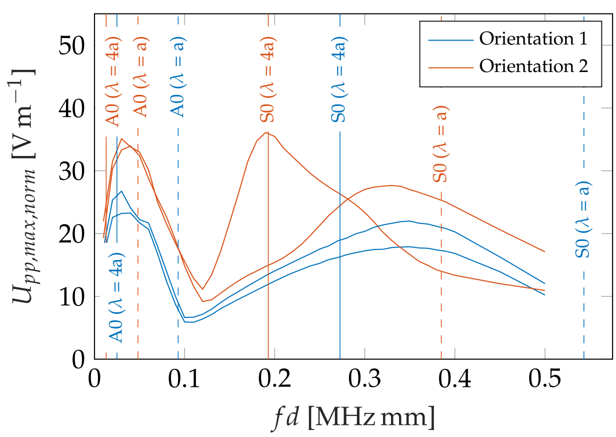

(b) Piezocomposite sensor: square, Figures 1c & 1d

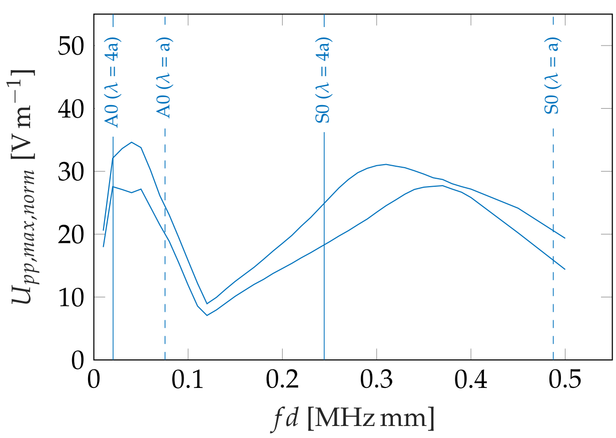

(c) Piezocomposite sensor: circle, Figure 1e

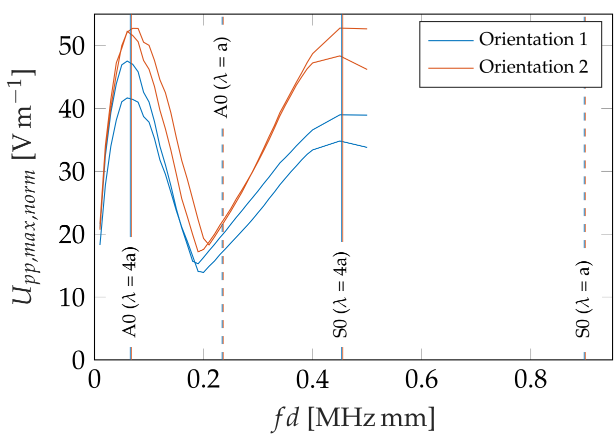

(d) Piezocomposite sensor: annulus segment, Figures 1f & 1g

Figure 3. Experimentally determined peak-to-peak voltage for different sensor types, shapes and orientations (see Figure 1) under GUW excitation in a 2 mm aluminum plate, analytically calculated amplitude maxima (solid vertical lines) and minima (dotted vertical lines) based on estimated effective sensor lengths in wave propagation direction (see Figure 1, Equations 2-3)

4. Conclusion

In this study, the detection of GUW in isotropic wave guides using tape casted piezoceramic composite sensors based on photopolymers is validated. This is experimentally shown for an isotropic aluminum plate with 2 mm thickness for frequencies of up to at least 250 kHz. Different sensor sizes and shapes show different sensitivities and although the sensitivity can not reach the one of solid PZT discs yet, further investigations might lead to advantageous sensors. To reach new forms of sensors the following research topics have to be addressed:

- Optimize the material properties to increase the piezoelectric sensitivity
- Extent research to other geometries
- Consider geometry rather than only referring to the estimated effective sensor length as a criterion
- Design a concept for variable, direction sensitive and mode selective sensors

Funding: The authors expressly acknowledge the financial support of the research work on this article within the Research Unit 3022 "Ultrasonic Monitoring of Fibre Metal Laminates Using Integrated Sensors" (Project number: 418311604) and the Research Project "Piezoelectric 0-0-3 Composites" (Project number: 389409970) by the German Research Foundation (Deutsche Forschungsgemeinschaft (DFG)).

Conflicts of Interest: The authors declare no conflict of interest. The funders had no role in the design of the study; in the collection, analyses, or interpretation of data; in the writing of the manuscript, or in the decision to publish the results.

References

1. Rose, J.L. *Ultrasonic guided waves in solid media*; Cambridge University Press: Cambridge, 2014. doi:10.1017/CBO9781107273610.
2. Schmidt, D. Modenselektive Übertragung von Lambwellen in Faserverbundstrukturen. Dissertation, Technische Universität Braunschweig, Braunschweig, 2014.
3. Lamb, H. On waves in an elastic plate. *Proceedings of the Royal Society of London. Series A, Containing Papers of a Mathematical and Physical Character* **1917**, *93*, 114–128. doi:10.1098/rspa.1917.0008.
4. Giurgiutiu, V. *Structural health monitoring with piezoelectric wafer active sensors*; Academic Press/Elsevier: Amsterdam, 2008.
5. Lammering, R.; Gabbert, U.; Sinapius, M.; Schuster, T.; Wierach, P., Eds. *Lamb-Wave Based Structural Health Monitoring in Polymer Composites*; Springer eBook Collection, Springer: Cham, 2018. doi:10.1007/978-3-319-49715-0.
6. PI Ceramic GmbH. Datasheet - Material Data of Piezoelectric Materials: Specific Parameters of the Standard Materials.
7. Giurgiutiu, V.; Lin, B. In-Situ Fabrication of Composite Piezoelectric Wafer Active Sensors for Structural Health Monitoring. Aerospace. ASMEDC, 2004, pp. 89–95. doi:10.1115/IMECE2004-60929.
8. Chen, Z.; Song, X.; Lei, L.; Chen, X.; Fei, C.; Chiu, C.T.; Qian, X.; Ma, T.; Yang, Y.; Shung, K.; Chen, Y.; Zhou, Q. 3D printing of piezoelectric element for energy focusing and ultrasonic sensing. *Nano Energy* **2016**, *27*, 78–86. doi:10.1016/j.nanoen.2016.06.048.
9. Cheng, J.; Chen, Y.; Wu, J.W.; Ji, X.R.; Wu, S.H. 3D Printing of BaTiO3 Piezoelectric Ceramics for a Focused Ultrasonic Array. *Sensors (Basel, Switzerland)* **2019**, *19*. doi:10.3390/s19194078.
10. Narita, F.; Fox, M. A Review on Piezoelectric, Magnetostrictive, and Magnetoelectric Materials and Device Technologies for Energy Harvesting Applications. *Advanced Engineering Materials* **2018**, *20*, 1700743. doi:10.1002/adem.201700743.
11. Sakamoto, W.K.; Higuti, R.T.; Crivelini, E.B.; Nagashima, H.N. Polymer matrix-based piezoelectric composite for structural health monitoring. 2013 Joint IEEE International Symposium on Applications of Ferroelectric and Workshop on Piezoresponse Force Microscopy (ISAF/PFM). IEEE, 2013, pp. 295–297. doi:10.1109/ISAF.2013.6748696.
12. Fang, X.; He, J.; Zhang, Y. Preparation and Characterization of Large-Area and Flexible Lead Zirconate Titanate/Polyvinyl-Butyral/Additives Composite Films for Piezoelectric Sensor Application. *Sensors and Materials* **2016**, *28*, 681–688. doi:10.18494/SAM.2016.1333.
13. Pan, H.H.; Huang, M.W. Piezoelectric cement sensor-based electromechanical impedance technique for the strength monitoring of cement mortar. *Construction and Building Materials* **2020**, *254*, 119307. doi:10.1016/j.conbuildmat.2020.119307.
14. Sirohi, J.; Chopra, I. Fundamental Understanding of Piezoelectric Strain Sensors. *Journal of Intelligent Material Systems and Structures* **2000**, *11*, 246–257. doi:10.1106/8BFB-GC8P-XQ47-YCQ0.
15. Mitkus, R.; Pierou, A.; Feder, J.; Sinapius, M. Investigation and Attempt to 3D Print Piezoelectric 0-3 Composites Made of Photopolymer Resins and PZT. ASME 2020 Conference on Smart Materials, Adaptive Structures and Intelligent Systems. American Society of Mechanical Engineers, 2020. doi:10.1115/SMASIS2020-2287.